www.czasopisma.pan.pl PAN www.journals.pan.pl
Opto-Electronics Review 25 (2017) 10–14

Contents lists available at ScienceDirect

Opto-Electronics Review

journal homepage: http://www.journals.elsevier.com/opto-electronics review

Tunable Q-switched ytterbium-doped fibre laser by using zinc oxide as saturable absorber

R.A. Shaharuddin [a], S.A. Azzuhri [a,*], M.A. Ismail [a], F.A.A. Rashid [a], M.Z. Samion [a], M.Z.A. Razak [b], H. Ahmad [a]

[a] Photonics Research Centre (PRC), University of Malaya, Kuala Lumpur, Malaysia
[b] Institute of Microengineering and Nanoelectronics, University Kebangsaan Malaysia, Selangor, Malaysia

ARTICLE INFO

Article history:
Available online 14 February 2017

Keywords:
Tunable Q-switched
ZnO
Tunable bandpass filter
Ytterbium

ABSTRACT

This paper demonstrates the use of a zinc oxide (ZnO) thin film in a 1-μm ring laser cavity as a saturable absorber to successfully generate Q-switching pulses. The tunability of the laser pulses is achieved by integrating a tunable bandpass filter (TBPF) in an ytterbium-doped laser cavity that results in 9.4 nm of tuning range, which wavelength is from 1040.70 nm to 1050.1 nm. The peak energy in the pulse which is 1.47 nJ was measured together with a minimum pulse width of 2.4 μs. In addition, the repetition rate increases from 25.77 to 45.94 kHz as the pump power level being increased from 103.1 to 175.1 mW. The results obtained in this experiment demonstrated consistent results and stable throughout the experiment. Therefore, ZnO thin film is considered as a good candidate in 1-μm pulsed laser applications.

1. Introduction

Since its invention in 1987, erbium-doped fibre amplifier (EDFA) has been widely used in broad area of application due to many advantages, such as low transmission loss, high gain, high optical efficiency and high saturation power [1–3]. However, there has been a growing interest in a 1-μm region using ytterbium-doped fibre laser (YDFL) because of its special properties, for example, high power efficiency, broad gain bandwidth, low quantum defect, flexible and compact [4–7].

In terms of Q-switching pulses generated in a 1-μm region, they are said to be more reliable with the existing of noise and pulse also spread gradually when the fibre loss exists compared to a 1.5-μm region [8]. Laser pulses have been used extensively in applications such as nonlinear optic, optical signal processing, excitonic absorption saturation and mechanical system controller [9–12]. Particularly, tunable Q-switched pulses generation using YDFL has sparked current research interest in applications such as spectroscopy and biomedical diagnostics [13] where the pulses can be adjusted to a different operating wavelength with ease which is the interest of this paper.

In general, there are two types of Q-switching generation methods which are active and passive techniques. Active Q-switching pulse method relies upon external electrically powered modulator to induce and to restore a high Q-factor in order to generate pulses [14]. On the other hand, passive Q-switching technique does not depend on any external signal but can use additional passive components such as saturable absorber (SA) material [14,15], semiconductor saturable absorber mirror (SESAM) [16], and nonlinear polarization rotation (NPR) [17] to induce pulses in the cavity.

Lately, there has been extensive works on Q-switch pulse laser generation using a different type of SA materials: carbon-based SAs such as single-walled (SW-) and multi-walled (MW-) carbon nanotubes (CNTs) [18], and graphene [19]; transition metal dichalcogenides (TMD) such as MoS2, MOSe2, WS2 [20–24]; topological insulator (TI) materials such as Bi2Te3, BiSe2, Bi2Se3m, Bi2Te3; black phosphorus; TiO2 have been demonstrated in various publications [25–27].

Various types of SA such as crystal SA and SESAMs can be used in order to cover various operation wavelengths [28–30]. In a 1-μm region, the use of SA materials such as graphene, Cr^{+3}:YAG, TI, TI:Ni_2Se_3, Molybdenum Disulfide (MoS_2) and tungsten disulfide (WS_2) has been reported in Q-switching pulses generation [5,31–35]. Recently, ZnO has been identified as a potential of a good SA since it exhibits a short recovery time and possesses a good saturable absorption [36]. There are few techniques that had been reported to achieve tunability in Q-switching operations, such as by inserting polarization controller (PC), TBPF or inserting both PC and TBPF in the laser cavity [37–39].

* Corresponding author.
E-mail address: saaidal@um.edu.my (S.A. Azzuhri).

http://dx.doi.org/10.1016/j.opelre.2017.01.002
1230-3402/

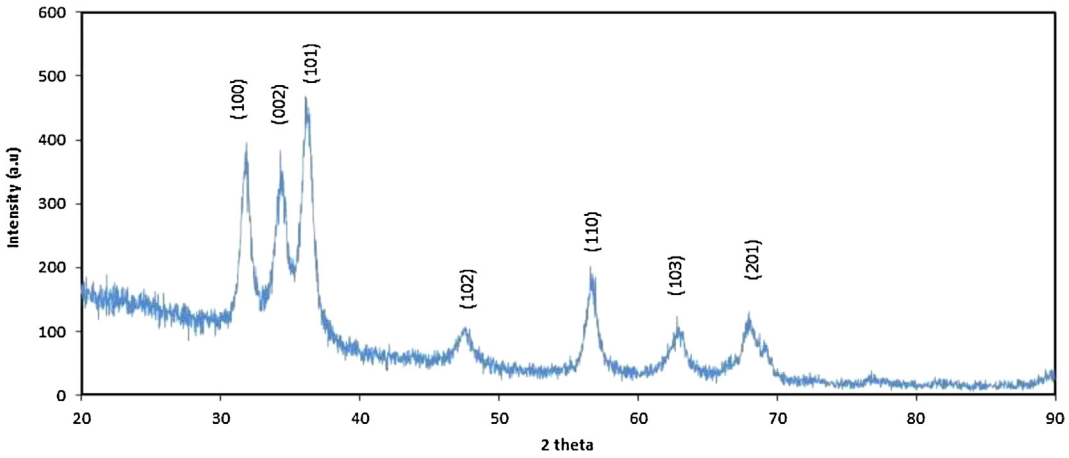

Fig. 1. ZnO nanoparticles XRD pattern [36].

In this paper, we have demonstrated the use of TBPF in the laser cavity between the isolator and the SA (ZnO) in order to investigate tunability of a Q-switching behaviour. A stable Q-switching operation with the tunability range of 9.4 nm covering from 1040.70 nm to 1050.1 nm was observed. In addition, the fabrication of ZnO has been well explained in this paper.

2. Zinc oxide saturable absorber characterization

The ZnO thin film SA used in the experiment was prepared by using a ZnO powder of 5 wt%. Firstly, the ZnO was prepared into a mixture by adding silane and ethanol with a ratio of 1:1 ethanol to silane [36]. Next, the mixture undergoes ultrasonification process for about 30 min. After that, sulphuric acids of 10 wt% were added into the mixture containing the ZnO, ethanol and silane. Next, the solution undergoes ultrasonification process for about 5 min. Lastly, the prepared mixture was then poured into a plastic mould and was set dry for three days at a room temperature.

Fig. 1 shows the result of X-ray diffraction (XRD) of the ZnO powder nanostructures. Each peak on the graph indicates that ZnO consists of a particle (nanoscale). Full-width at half maximum (FWHM) data, peak intensity and, position and width can be determined based on the XRD patterns analysis [26]. Each planes, ⟨1 0 0⟩, ⟨0 0 2⟩, ⟨1 0 1⟩, ⟨1 0 2⟩, ⟨1 1 0⟩, ⟨1 0 3⟩, and ⟨2 0 1⟩ correspond to different diffraction peaks. The result confirmed the existence of a ZnO peak as it shows no characteristics of XRD peaks. Thus, it proves that no impurities exist in the synthesized nanopowder.

To analyze the absorption and modulation depth of ZnO, an experimental set-up shown in Fig. 2(a) was utilized. A laser diode pump with an output wavelength of 974 nm was connected to a wavelength division multiplexer (WDM) and, subsequently, connected to an erbium-doped fibre (EDF) gain medium. In order to ensure unidirectional lasing in the cavity, an isolator is used in the ring cavity. Then, the isolator was connected to a fibre ferrule that contains the SA, which is a piece of CNT thin film that is used to generate a pulse seed source. Generating a pulse seed source using the CNT film is crucial in order to induce mode lock pulses for the measurement. The mode lock pulses were then amplified by using self-assemble EDFA in order to produce maximum peak power that covering 1550 nm region (the S, C and L band) [40–42].

The high peak power pulses generated using the CNT SA are then used to saturate the ZnO sample. In order to do this, the high power output pulses, which are about 10 dB, were channelled thru a variable optical attenuator (VOA) to gradually vary the power level. The signal pulses were attenuated from 0 dB to −60 dB by using the VOA with a 1 dB step. A 3 dB optical coupler (OC2) is connected to

(a)

$$\alpha = \frac{\Delta\alpha}{\left(1+\frac{I}{I_{sat}}\right)} + \alpha_{linear} \quad \text{..... (1)}$$

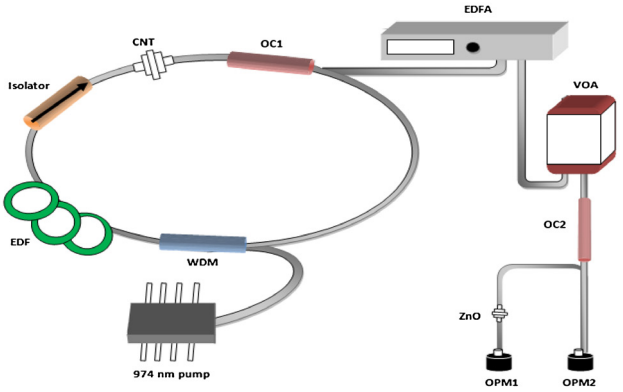

(b)

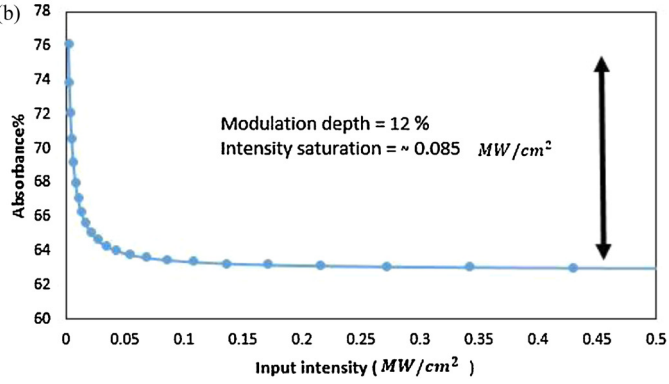

Fig. 2. (a) Cavity design to measure nonlinear absorption of ZnO, (b) saturable absorption characteristic of ZnO.

the VOA to split the signal equally into two parts. One part of the output of the OC2 acts as a reference and is connected to the optical power meter (OPM1). On the other hand, another output of the OC2 passes through a connector containing the ZnO thin film. The SA is put between two fibre ferrules. The fibre ferrule is then connected the second OPM (OPM2) for comparison.

The magnitude difference between readings of OPM1 and OPM2 was analyzed to measure the modulation depth of the ZnO. By using Eq. (1), the calculated modulation depth was found nearly 36%,

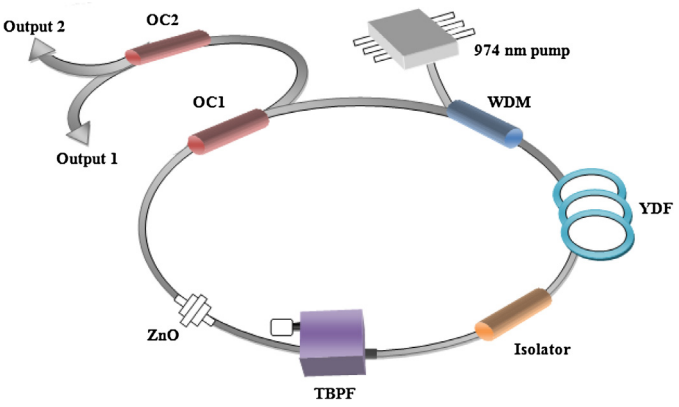

Fig. 3. Ring cavity design for tunable Q-switch YDFL.

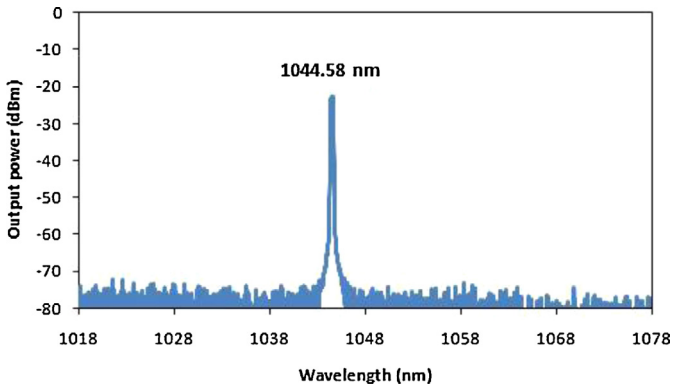

Fig. 4. Optical spectrum analyzer at 1044.58 nm.

while the saturation intensity is approximately of ~0.01 MW/cm^2. The analyzed data is represented in the graph as shown in Fig. 2(b)

$$\alpha = \frac{\Delta\alpha}{(1 + I/I_{sat})} + \alpha_{linear}. \quad (1)$$

3. Laser cavity design

Fig. 3 shows a laser in a cavity setup for a tunable Q-switching YDFL. A laser diode with a pumping wavelength at 974 nm is connected to a WDM. The maximum output power of the laser diode is of 450 mW. In this cavity, YDF is used as the gain media for the continuous wave (CW) laser generation. The YDF with a length of 70 cm is connected between 980/1060 nm WDM and a polarization independent isolator (Isolator). The function of the isolator is to ensure that there is no reflection in the ring cavity by allowing only unidirectional light propagation. The other end of the isolator is connected to a tunable bandpass filter (TBPF). The reason of using the TBPF in this laser cavity is to adjust the bandwidth to deliver the output as a function of the fundamental frequency of an input signal. The TBPF is fine-tuned to peak at the specific wavelength without distorting the Q-switching pulses. The fibre ferrule containing the SA is then connected to the tunable bandpass filter (TBPF).

In this work, a single layer zinc oxide (ZnO) thin film is used and sandwiched between the fibre ferrules. A 90:10 optical coupler is connected to the fibre ferrules containing the SA film, where the ferrules were located in between the coupler and the TBPF. The 10 percent output port is drawn from the first optical coupler (OC1) and it was then fixed to another 50:50 optical coupler (OC2) to split the output of the OC1 equally. The 3 dB coupler was included to monitor the result using an optical spectrum analyzer (OSA) and

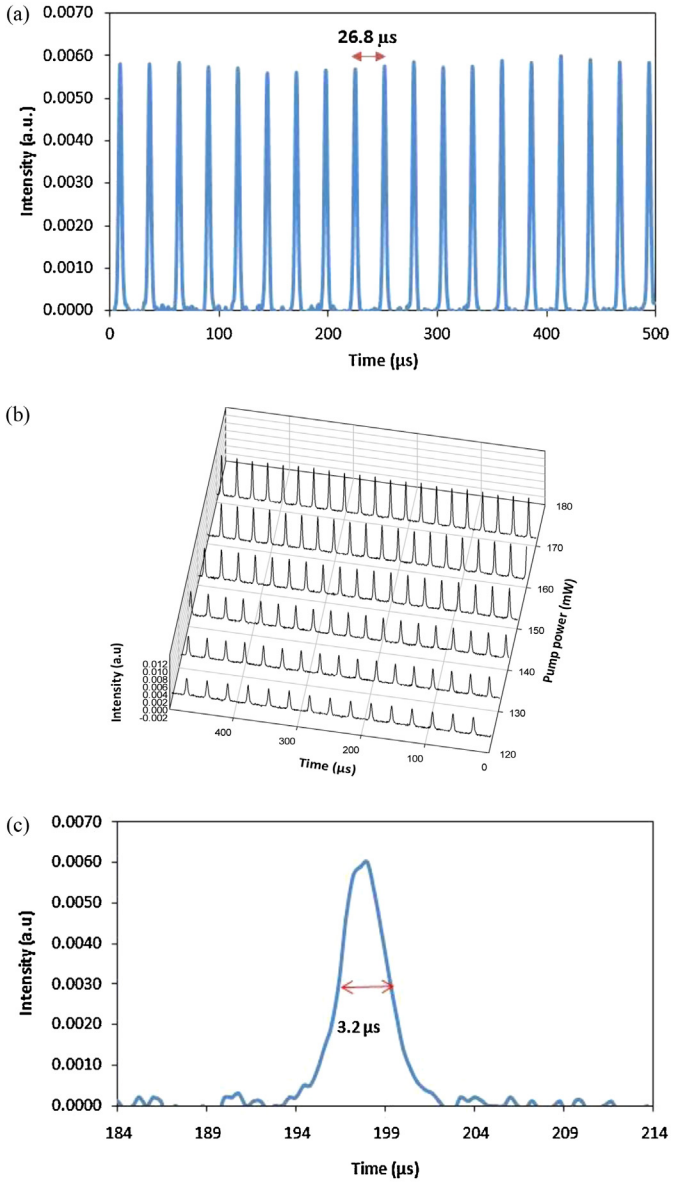

Fig. 5. (a) Q-switched pulse train at 145.9 mW, (b) Pulse train of Q-switched ZnO at pump power 122.1 mW until 170.1 mW within 500 µs duration, and (c) pulse width at 145.9 mW pump power.

an oscilloscope simultaneously. Meanwhile, the other output port (90%) of the OC1 is looped back into the ring cavity.

4. Results and discussion

The result in Fig. 4 shows the lasing threshold for the Q-switched pulses at the OSA. This result corresponds to the pump power of 103.1 mW at input. The peak wavelength is located at 1044.6 nm with an output power of –20.26 dBm.

In this experiment, the stable Q-switched pulses started to appear at 103.1 mW of the pump power level and the pulses diminished after the power level exceeding 175.1 mW. The output data was obtained using the oscilloscope through a photodetector that convert the light output for the measurement. The photodetector converts light signal into electrical signal according to the principle of photoelectric effect. The result of the Q-switched pulse train at the pump power of 145.9 mW is shown in Fig. 5(a) while Fig. 5(b) shows the graph of the pulse train for the Q-switching pulses measured with different input power levels. In this graph,

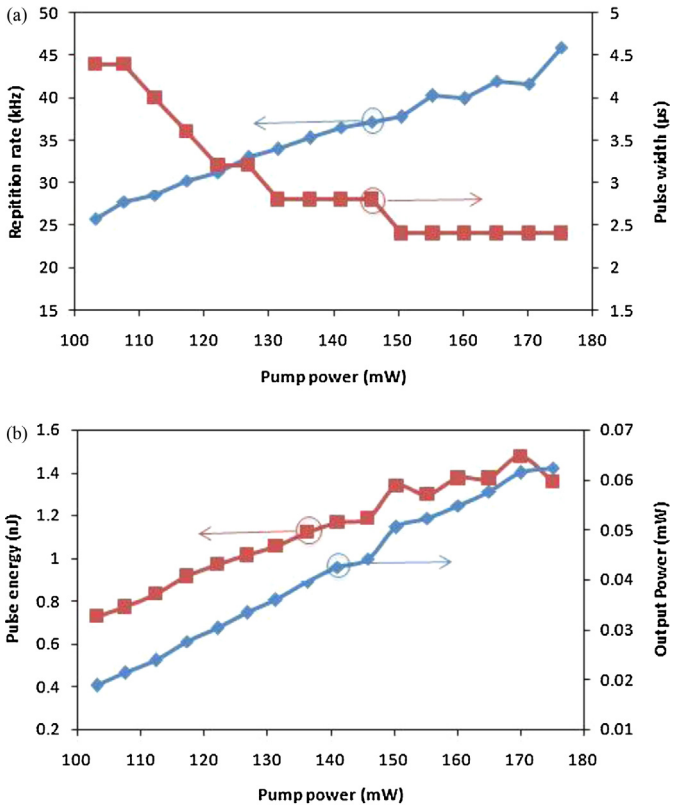

Fig. 6. (a) Repetition rate and pulse width *vs.* pump power and (b) peak power and pulse energy *vs.* pump power before tuning the TBPF.

the pump power level is increased from 122.1 mW to 170.1 mW and the results are observed. As the pump power increased, both magnitude and the repetition rate of the pulses also increased indicate the Q-switching behaviour.

There are four important criteria when analyzing Q-switching results: they are the repetition rate, the pulse width, the peak power, and the pulse energy, all against variation of the pump power. The results of the Q-switching performance according to these criteria are illustrated in Fig. 6. In Fig. 6(a), the repetition rate and the pulse width *vs.* laser diode pump power are illustrated. With the increment of the pump power from 103.1 mW to 175.1 mW, the repetition rate increases accordingly from 25.77 kHz to 45.94 kHz. This phenomenon confirmed the behaviour of the Q-switched characteristics [30]. On the contrary, a decreasing trend

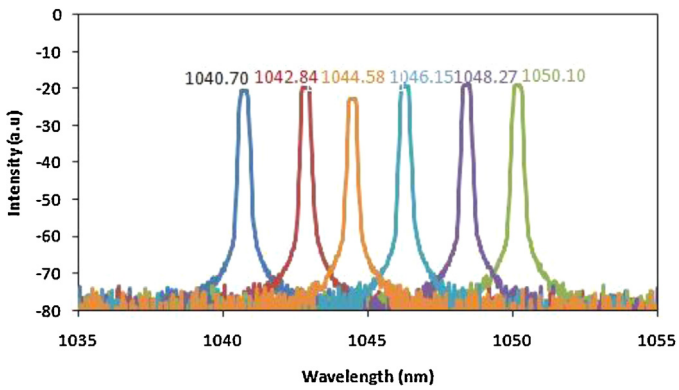

Fig. 8. Tunability of Q-switch operation from 1040.70 nm to 1050.1 nm at pump power 145.9 mW.

of the pulse width from 4.4 μs to 2.4 μs could be observed as the pump power is increased with the same amount. Therefore, the observed results have confirmed that the proposed set-up behaving the Q-switching characteristics as the repetition rates increases with the increment of the pump power levels while the pulse width and the pulse duration decreases as the pump power increased.

Fig. 6(b) shows the result of the pulse energy against the pump power as indicated by the red line while the blue line indicates the peak power *vs.* the pump power. In this graph, both lines show increasing trends upon the increment of the pump power from 103.1 mW to 170.1 mW but fall slightly after 170.1 mW. The maximum energy recorded for single Q-switched pulses is of 1.47 nJ and the minimum pulse width is of 2.4 μs.

Radio frequency spectrum analyzer (RFSA) is used to validate the trace results measured in the frequency domain. The result of the RFSA spectrum is illustrated in Fig. 7. In addition, a full half-width measurement (FHWM) is the method used to measure the pulse width. The pulse width of RF spectrum measured is of 3.2 μs. The fundamental frequency is measured at 145.9 mW of the pump power and the repetition rate of 37.19 kHz is proven by the RFSA spectrum. Meanwhile, the peak-to-pedestal ratio (PPR) of 31.2 dB is obtained in this experiment as presented in Fig. 7.

The tunability of the Q-switched is obtained by tuning the passband of the TBPF, resulting a tunability range of 9.4 nm, measured from 1040.70 nm until 1050.1 nm as indicated in Fig. 8. A steady pulse train is achieved throughout the tunability process. The pump power is kept constant at 145.9 mW upon taking the reading. Stable Q-switched pulses are observed starting at a wavelength of 1040.70 nm and diminish after 1050.10 nm. We believed such small

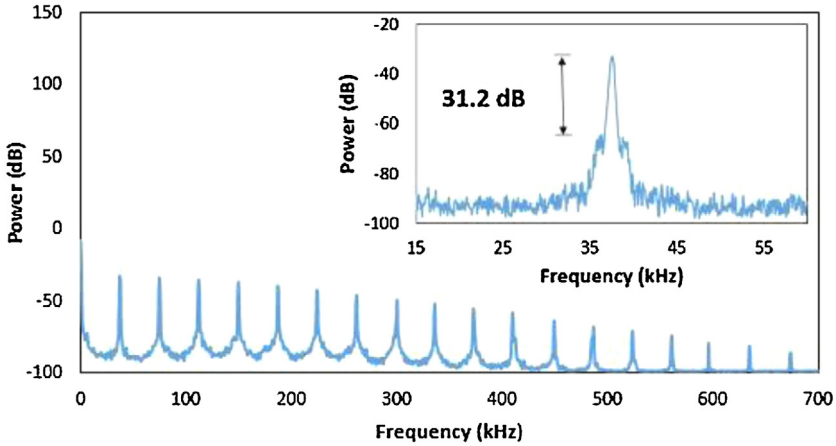

Fig. 7. RF spectrum.

margin is due to a high gain bandwidth of the gain medium (YDF) instead of the SA [36,43].

5. Conclusions

In this paper, a tunable Q-switched ZnO operating in a 1-μm region has been successfully demonstrated. A single layer of ZnO thin film with a dimension of 1 mm × 1 mm has been used in this experiment. A stable Q-switched started to appear at a pump power of 103.1 mW at a wavelength of 1044.58 nm. To achieve the tunability, a TBPF was introduced into the ring cavity. The Q-switched is tuned from 1040.70 nm to 1050.1 nm with the total tunable range of 9.4 nm. In this experiment, the maximum energy recorded for a single Q-switched pulse is of 1.47 nJ and the minimum pulse width is of 2.4 μs. Meanwhile, the repetition rate of the pulses is measured between 25.77 and 45.94 kHz. Based on the results obtained from this experiment, we conclude that ZnO thin film has potential to be used in a stable pulsed laser generation including in the applications of biomedical diagnostic and spectroscopy.

Acknowledgements

We thank the University of Malaya for supporting this work, which was funded by research grant nos. GA010-2014 (ULUNG), RU007/2015, UM.C/625/1/HIR/MOHE/SCI/29, LRGS (2015)/NGOD/UM/KPT and BR002-2016.

References

[1] W.J. Miniscalco, Erbium-doped glasses for fibre amplifiers at 1500 nm, J. Lightwave Technol. 9 (1991) 234–250.
[2] P.M. Becker, A.A. Olsson, J.R. Simpson, Erbium-Doped Fibre Amplifiers: Fundamentals and Technology, Academic Press, 1999.
[3] B.J. Ainslie, A review of the fabrication and properties of erbium-doped fibres for optical amplifiers, J. Lightwave Technol. 9 (1991) 220–227.
[4] V. Durairaj, Amplification in Ytterbium-Doped Fibres (thesis), 2013.
[5] Z. Luo, Y. Huang, J. Weng, H. Cheng, Z. Lin, B. Xu, et al., 1.06 μm Q-switched ytterbium-doped fibre laser using few-layer topological insulator Bi_2Se_3 as a saturable absorber, Opt. Express 21 (2013) 29516–29522.
[6] R. Paschotta, J. Nilsson, A.C. Tropper, D.C. Hanna, Ytterbium-doped fibre amplifiers, IEEE J. Quant. Electron. 33 (1997) 1049–1056.
[7] P.J. Suni, D.C. Hanna, R. Percival, I.R. Perry, R.G. Smart, J.E. Townsend, et al., Lasing characteristics of ytterbium, thulium and other rare-earth doped silica based fibres, in: OE/FIBRES'89, 1990, pp. 244–260.
[8] G. Agrawal, Applications of Nonlinear Fibre Optics, Academic Press, 2010.
[9] G. Stegeman, D. Hagan, L. Torner, $\chi^{(2)}$ cascading phenomena and their applications to all-optical signal processing, mode-locking, pulse compression and solitons, Opt. Quant. Electron. 28 (1996) 1691–1740.
[10] P.W. Smith, D.A. Miller, Y. Silberberg, Mode locking of semiconductor diode lasers using saturable excitonic nonlinearities, JOSA B 2 (1985) 1228–1236.
[11] J.J. Zayhowski, Passively Q-switched Nd:YAG microchip lasers and applications, J. Alloys Compd. 303 (2000) 393–400.
[12] D. Liberzon, A.S. Morse, Basic problems in stability and design of switched systems, IEEE Control Syst. 19 (1999) 59–70.
[13] R.I. Woodward, E.J. Kelleher, R.C. Howe, G. Hu, F. Torrisi, T. Hasan, et al., Tunable Q-switched fibre laser based on saturable edge-state absorption in few-layer molybdenum disulfide [MoS(2)], Opt. Express 22 (2014) 31113–31122.
[14] M. Eichhorn, Generation of short and ultra-short pulses, in: Laser Physics, Springer, 2014, pp. 75–103.
[15] A. Malyarevich, I. Denisov, K. Yumashev, V. Mikhailov, R. Conroy, B. Sinclair, V:YAG – a new passive Q-switch for diode-pumped solid-state lasers, Appl. Phys. B: Laser Opt. 67 (1998) 555–558.
[16] R. Fluck, B. Braun, E. Gini, H. Melchior, U. Keller, Passively Q-switched 1.34-μm Nd:YVO_4 microchip laser with semiconductor saturable-absorber mirrors, Opt. Lett. 22 (1997) 991–993.
[17] X. Feng, H.-y. Tam, P. Wai, Stable and uniform multiwavelength erbium-doped fibre laser using nonlinear polarization rotation, Opt. Express 14 (2006) 8205–8210.
[18] S.Y. Set, H. Yaguchi, Y. Tanaka, M. Jablonski, Laser mode locking using a saturable absorber incorporating carbon nanotubes, J. Lightwave Technol. 22 (2004) 51–56.
[19] Q. Bao, H. Zhang, Y. Wang, Z. Ni, Y. Yan, Z.X. Shen, et al., Atomic-layer graphene as a saturable absorber for ultrafast pulsed lasers, Adv. Funct. Mater. 19 (2009) 3077–3083.
[20] K. Wang, J. Wang, J. Fan, M. Lotya, A. O'Neill, D. Fox, et al., Ultrafast saturable absorption of two-dimensional MoS_2 nanosheets, ACS Nano 7 (2013) 9260–9267.
[21] B. Chen, X. Zhang, K. Wu, H. Wang, J. Wang, J. Chen, Q-switched fibre laser based on transition metal dichalcogenides MoS2, MoSe2, WS2, and WSe2, Opt. Express 23 (2015) 26723–26737.
[22] C. Zhao, H. Zhang, X. Qi, Y. Chen, Z. Wang, S. Wen, et al., Ultra-short pulse generation by a topological insulator based saturable absorber, Appl. Phys. Lett. 101 (2012) 211106.
[23] K. Wu, X. Zhang, J. Wang, X. Li, J. Chen, WS2 as a saturable absorber for ultrafast photonic applications of mode-locked and Q-switched lasers, Opt. Express 23 (2015) 11453–11461.
[24] Z. Luo, Y. Huang, M. Zhong, Y. Li, J. Wu, B. Xu, et al., 1-, 1.5-, and 2-μm fibre lasers Q-switched by a broadband few-layer MoS_2 saturable absorber, J. Lightwave Technol. 32 (2014) 4077–4084.
[25] Y. Chen, C. Zhao, H. Huang, S. Chen, P. Tang, Z. Wang, et al., Self-assembled topological insulator: BiSe membrane as a passive Q-switcher in an erbium-doped fibre laser, J. Lightwave Technol. 31 (2013) 2857–2863.
[26] P. Tang, X. Zhang, C. Zhao, Y. Wang, H. Zhang, D. Shen, et al., Topological insulator: saturable absorber for the passive Q-switching operation of an in-band pumped 1645-nm Er:YAG ceramic laser, IEEE Photon. J. 5 (2013) 1500707.
[27] J. Lee, J. Koo, Y.M. Jhon, J.H. Lee, A femtosecond pulse erbium fibre laser incorporating a saturable absorber based on bulk-structured Bi2Te3 topological insulator, Opt. Express 22 (2014) 6165–6173.
[28] R. Paschotta, R. Häring, E. Gini, H. Melchior, U. Keller, H. Offerhaus, et al., Passively Q-switched 0.1-mJ fibre laser system at 1.53 nm, Opt. Lett. 24 (1999) 388–390.
[29] Y. Bai, N. Wu, J. Zhang, J. Li, S. Li, J. Xu, et al., Passively Q-switched Nd:YVO_4 laser with a Cr^{4+}:YAG crystal saturable absorber, Appl. Opt. 36 (1997) 2468–2472.
[30] F.Z. Qamar, T.A. King, Passive Q-switching of the Tm-silica fibre laser near 2 μm by a Cr^{2+}:ZnSe saturable absorber crystal, Opt. Commun. 248 (2005) 501–508.
[31] Z. Luo, M. Zhou, J. Weng, G. Huang, H. Xu, C. Ye, et al., Graphene-based passively Q-switched dual-wavelength erbium-doped fibre laser, Opt. Lett. 35 (2010) 3709–3711.
[32] J. Huang, H. Liang, K. Su, Y.-F. Chen, High power passively Q-switched ytterbium fibre laser with Cr^{4+}:YAG as a saturable absorber, Opt. Express 15 (2007) 473–479.
[33] J. Liu, S. Wu, Q.-H. Yang, P. Wang, Stable nanosecond pulse generation from a graphene-based passively Q-switched Yb-doped fibre laser, Opt. Lett. 36 (2011) 4008–4010.
[34] M. Zhang, G. Hu, G. Hu, R. Howe, L. Chen, Z. Zheng, et al., Yb-and Er-doped fibre laser Q-switched with an optically uniform, broadband WS2 saturable absorber, Sci. Rep. 5 (2015).
[35] J. Du, Q. Wang, G. Jiang, C. Xu, C. Zhao, Y. Xiang, et al., Ytterbium-doped fibre laser passively mode locked by few-layer molybdenum disulfide (MoS_2) saturable absorber functioned with evanescent field interaction, Sci. Rep. 4 (2014).
[36] H. Ahmad, C. Lee, M. Ismail, Z. Ali, S. Reduan, N. Ruslan, et al., Tunable Q-switched fibre laser using zinc oxide nanoparticles as a saturable absorber, Appl. Opt. 55 (2016) 4277–4281.
[37] W. Cao, H. Wang, A. Luo, Z. Luo, W. Xu, Graphene-based, 50 nm wide-band tunable passively Q-switched fibre laser, Laser Phys. Lett. 9 (2011) 54.
[38] D. Popa, Z. Sun, T. Hasan, F. Torrisi, F. Wang, A. Ferrari, Graphene Q-Switched Tunable Fibre Laser, 2010 arXiv:1011.0115.
[39] D.-P. Zhou, L. Wei, B. Dong, W.-K. Liu, Tunable passively-switched erbium-doped fibre laser with carbon nanotubes as a saturable absorber, IEEE Photon. Technol. Lett. 22 (2010) 9–11.
[40] S. Harun, F. Abd Rahman, K. Dimyati, H. Ahmad, An efficient gain-flattened C-band Erbium-doped fibre amplifier, Laser Phys. Lett. 3 (2006) 536–538.
[41] H. Ahmad, N. Saat, S. Harun, S-band erbium-doped fibre ring laser using a fibre Bragg grating, Laser Phys. Lett. 2 (2005) 369.
[42] H. Ahmad, S. Shahi, S. Harun, Bismuth-based erbium-doped fibre as a gain medium for L-band amplification and Brillouin fibre laser, Laser Phys. 20 (2010) 716–719.
[43] R. Woodward, E. Kelleher, R. Howe, G. Hu, F. Torrisi, T. Hasan, et al., Tunable Q-switched fibre laser based on saturable edge-state absorption in few-layer molybdenum disulfide (MoS2), Opt. Express 22 (2014) 31113–31122.